DENTAL MATERIALS 35 (2019) 1718–1727

Available online at www.sciencedirect.com

ScienceDirect

journal homepage: www.intl.elsevierhealth.com/journals/dema

Morphological and elemental analysis of silver penetration into sound/demineralized dentin after SDF application

Mahmoud Sayed[a,*], *Naoko Matsui*[a,*], *Motohiro Uo*[b,c], *Toru Nikaido*[d], *Masakazu Oikawa*[e], *Michael F. Burrow*[f], *Junji Tagami*[a]

[a] *Department of Cariology and Operative Dentistry, Graduate School of Medical and Dental Sciences, Tokyo Medical and Dental University, Tokyo, Japan*

[b] *Department of Advanced Biomaterials, Graduate School of Medical and Dental Sciences, Tokyo Medical and Dental University, 1-5-45, Yushima, Bunkyo-ku, Tokyo, Japan*

[c] *Department of Materials Engineering, Graduate School of Engineering, The University of Tokyo, 7-3-1, Hongo, Bunkyo-ku, Tokyo, Japan*

[d] *Department of Operative Dentistry, Division of Oral Functional Science and Rehabilitation, School of Dentistry, Asahi University, Gifu, Japan*

[e] *National Institute of Radiological Sciences, 4-9-1 Anagawa, Inage-ku, Chiba 263-8555, Japan*

[f] *University of Hong Kong, Faculty of Dentistry, Hong Kong SAR, China*

ARTICLE INFO

Keywords:
Silver diammine fluoride
Silver penetration
Discoloration
Micro-PIXE/PIGE
Dentin

ABSTRACT

Objective. The aim of this study was to evaluate the penetration depth of silver into sound and demineralized dentin after application of silver diamine fluoride (SDF).

Methods. Two hundred and eighty-eight dentin specimens were used. The specimens were divided into 3 groups: (1) sound dentin (control), (2) 30 min EDTA-treated dentin; and (3) 13 h EDTA-treated dentin. SDF was applied to all specimens. Each group was divided into 3 subgroups according to storage time into: 24 h, 2 weeks and 1-year storage time. Each subgroup was further divided into four subgroups (n = 8) according to different examinations as optical microscope (OM) observation, scanning electron microscopic (SEM) observation, elemental analysis with energy dispersive spectroscopy (EDS) and Micro-PIXE test.

Results. The OM showed discoloration in the superficial layer after 24 h and keep extending deeper after 2 weeks and 1-year. SEM showed silver crystals within dentinal tubules after 2 weeks and 1-year. EDS analysis can detect silver penetration only in the 1-year group reaching around 1200 μm inside dentin. Micro-PIXE test detected silver at all time intervals, confirming the EDS depth results.

Significance. It can be concluded that silver ions can completely infiltrate the demineralized dentin lesion with further penetration into the underlying mineralized dentin.

* Corresponding authors at: Cariology and Operative Dentistry, Graduate School of Medical and Dental Sciences, Tokyo Medical and Dental University, 1-5-45, Yushima, Bunkyo-ku, 113-8549, Tokyo, Japan.

E-mail addresses: Drmahmoudmacklad@gmail.com (M. Sayed), Matsui.ope@gmail.com (N. Matsui).

https://doi.org/10.1016/j.dental.2019.08.111

1. Introduction

The minimal intervention philosophy principally promotes preservation of tooth structure, and, therefore places prevention and arresting dental caries as the first line of management of the disease [1]. Currently, studies are focusing on improving the antibacterial properties of biomaterials by using elements such as silver. Several antimicrobial dental products based on silver have been studied, including dental adhesives, silver-doped hydroxyapatite and primers [2].

Silver (Ag) has a long history of use in both the medical and dental fields since the 1800s because of its antimicrobial and anti-caries properties [3]. The combination of silver and fluoride was advocated for the combined beneficial effects of being anti-microbial and potentially aiding remineralization of teeth affected by dental caries [4]. In the late 1960s, silver diammine fluoride (SDF) was introduced in Japan. It showed good chemical stability compared with previous silver fluoride compounds [5]. Recently, the United States Food and Drug Administration approved the clinical use of SDF as it matches the goals for 21st century medical care of the World Health Organization [4].

SDF increases the resistance of tooth structures against demineralization, is believed to enhance remineralization [6] and reduces the formation of biofilm on tooth surfaces [7]. The potent anti-bacterial action of SDF against cariogenic bacteria has been attributed to the presence of silver ions [8].

SDF is considered a simple, non-invasive and cost-effective treatment modality to arrest dental caries [9,10]. However, it still has several unwanted effects including discoloration [4,11] and potential pulpal irritation [12] due to penetration and deposition of silver particles within dentinal tubules and its high pH. In addition, the high concentration of Ag ions in SDF may affect the conformation of dentin collagen [13,14].

In order to more fully understand the reaction behavior between SDF and dentin, the distribution of silver (Ag) and fluorine (F), which are the major elements within SDF, should be visualized. The scanning electron microscope-based elemental analysis methods (e.g. X-ray micro analysis (XMA) or SEM-energy dispersed spectroscopy (SEM/EDS)) are commonly used to determine the elemental distribution within a material. However, the sensitivity for Ag and F analysis with the above methods has a low resolution, therefore, making identification and analysis of the ionic distribution throughout dentin difficult analyze. Micro-focused particle induced X-ray emission (PIXE) and particle induced gamma-ray emission (PIGE) analysis uses the characteristic X-rays and γ-rays generated by accelerated protons (or charged particles) to detect elements. PIXE has a high sensitivity especially for 'heavy' elements, e.g. Ag. [15,16]. Fluorine is a 'light' element and difficult to detect using characteristic X-rays, because the characteristic X-ray of F is of low energy. However, PIGE detects the prompt γ-rays (which have much higher energy at around 110 keV) generated from F. Therefore, F could be effectively detected by PIGE [17]. PIXE and PIGE can be undertaken simultaneously by using different detectors for X-rays and γ-rays. Therefore, micro-PIXE/PIGE were applied to reveal Ag, F and the distribution of other elements in dentin.

Thus, the aim of this study was to evaluate the penetration depth of silver into sound and demineralized dentin after the application of 38% SDF and the relationship between silver penetration and discoloration. The null hypothesis was that silver can only penetrate demineralized bovine dentin without penetrating further into the underlying sound dentin.

2. Materials and methods

2.1. Specimens preparation

A total of 288 bovine dentin specimens were used in this study. The specimens (6 × 6 × 2 mm) were prepared from the cervical portion of the bovine incisor root. Specimens with cracks or showing heavy cervical tooth loss and sclerosis were excluded. Teeth were cut horizontally at the cemento-enamel junction to separate the crown from the root portion, then the root was cut vertically to obtain dentin specimens from the buccal and lingual surfaces of cervical portion using a low-speed diamond saw (Isomet 1000, Buehler, Lake Bluff, IL, USA) under copious water coolant. The surfaces of the specimens were ground using a series of silicon carbide papers (SiC) (600–2,000-grit, Fuji Star, Sankyo Rikagaku, Saitama, Japan) under running water to flatten the dentin surface, then ultra-sonicated in deionized water (DW) (Milli-Q water; Millipore, Billerica, MA, USA) for 3 min.

The specimens were randomly divided into three groups: the first group received no treatment (control), while the remaining two groups were demineralized with 0.5 M ethylene diamine tetra-acetic acid adjusted to pH 7.5 (EDTA: Decalcifying Soln. B, Wako Pure Chemical Industries, Osaka, Japan) for either 30 min or 13 h, respectively (EDTA 30 min and EDTA 13 h), and then rinsed in distilled water for 10 s. A swept-source optical coherence tomography (SS-OCT) system (IVS-2000, Santec, Komaki, Japan) was used to assess the depth of dentin demineralization treated with the EDTA solution. Mean lesion depths were confirmed at 80 ± 2.5 μm for the 30 min EDTA-treated group and 200 ± 3.5 μm for the 13 h EDTA-treated group, respectively.

Thirty-eight percent silver diammine fluoride (SDF) (Saforide, Bee Brand Medico Dental, Osaka, Japan) was applied to dentin surfaces for 1 min with agitation using a microbrush, then left for 2 min and rinsed with distilled water for 30 s.

Each group was divided into 3 subgroups according to storage time: 24 h, 2 weeks and 1-year. Each subgroup was further divided into a further four groups (n = 8) according to different microscopic evaluations, namely light microscope observation, scanning electron microscopy (SEM), elemental analysis with energy dispersive spectroscopy (EDS) and micro-PIXE/PIGE analysis. All specimens were stored at 100% relative humidity using wet tissue paper (renewed every week) and incubated at 37 °C during the time of the experiment. (Fig. 1)

2.2. Light microscope observation

After the storage periods, specimens were sectioned along the long axis of the tooth into two halves using a diamond blade (Isomet). The exposed cross-sectional surfaces were polished

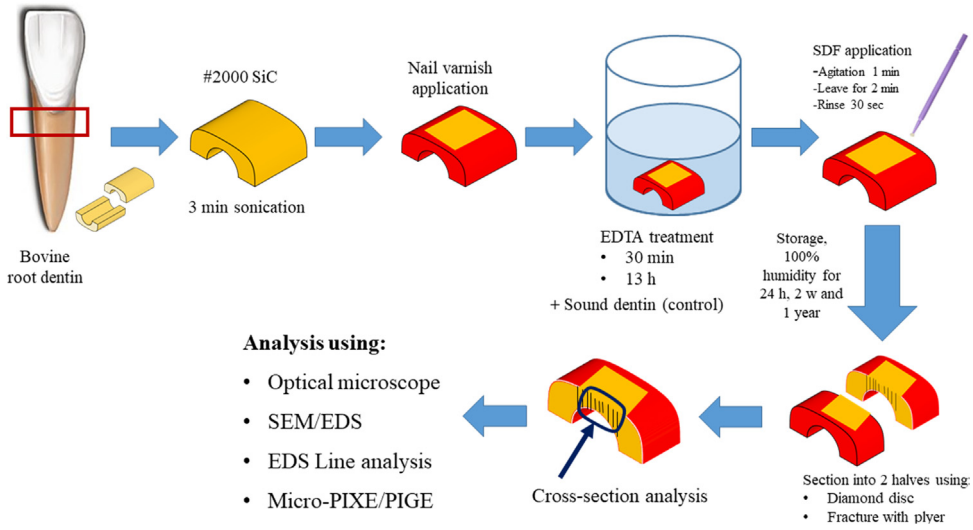

Fig. 1 – Illustration of specimen preparation. N = 8 for each analytical step.

using 600–2,000-grit SiC papers under running water and sonicated in distilled water for 3 min to remove the smear layer. Then the specimens were observed using a light microscope (LM, Nikon SMZ1000, Nikon Corp., Tokyo, Japan) at 3× magnification to determine the depth of discoloration.

2.3. *SEM/EDS point analysis observation*

After the three storage periods (24 h, 2 weeks and 1-year), the specimens were fixed using 2.5% glutaraldehyde for 2 h at 4 °C for primary fixation, followed with 0.1% osmium tetroxide solution for 2 h at 4 °C for secondary fixation then dehydrated in ascending concentrations of ethanol (50%, 70%, 80%, 90% and 95% for 25 min each; then, twice in 100% for 25 min each). [18]

Prior to sputter-coating with osmium tetroxide (4 nm layer thickness), each specimen was fractured down the middle with pliers along a pre-prepared groove. The fractured surfaces were observed using a field emission scanning electron microscope (SEM) (FE-SEM, S-4500, Hitachi Ltd., Tokyo, Japan) with operating conditions of 15 kV. Elemental point analysis for the fractured surfaces of the specimens was undertaken to detect the presence and distribution of phosphorous (P), calcium (Ca) and silver (Ag) ions via energy dispersive X-ray spectroscopy (EDS).

2.4. *Elemental line analysis with EDS*

After each storage time, a further set of specimens was embedded in polymethymethacrylate (Unifast III, GC, Tokyo, Japan) and sectioned along the long axis of the tooth into two halves using diamond blade (Isomet). The exposed cross-sectional surfaces were treated with 1% acetic acid for 5 s and washed with ultra-sonication in distilled water [13]. The specimens were sputter-coated with carbon. Lines were randomly selected from the surface of the specimen towards the pulp.

Elemental analysis was performed to identify calcium (Ca), phosphorous (P) and silver (Ag) ions via EDS under SEM (JSM-IT100 SEM, JEOL Ltd., Tokyo, Japan) with operating conditions of 15 kV.

2.5. *Micro-PIXE/PIGE analysis*

Stored specimens, for the two time periods, were sectioned to a thickness of approximately 0.5 mm using a low-speed diamond saw (Isomet) using water coolant. The sectioned specimens were polished to a thickness of less than 100 μm (Speed Rap ML-521-d, Maruto Instrument CO, Tokyo, Japan). Following this, the polished SDF-treated dentin was prepared for the Micro-PIXE analyses that were conducted at the National Institute of Radiological Sciences (Chiba, Japan). An accelerated micro-focused proton beam (3.0 MeV, 2 μm beam diameter) with raster scanning was applied over the target area of the specimen (maximum area 1.2 × 1.2 mm). The generated characteristic X-rays and prompt γ-rays from F (110 keV) were collected using Si (Li) and CdTe detectors to obtain the elemental distribution images and the characteristic X-ray/γ-ray spectra. The obtained data were processed with analysis software (OMDAQ2007, Oxford Microbeams, Bicester, UK), and the elemental distribution images were generated. The cumulative depth profiles of F, Ca, and Ag were calculated by using image analysis software (ImageJ, Ver1.46 r, National Institutes of Health, USA) from each elemental distribution image. Smoothing of the depth profile of F was applied to suppress the noise because the γ-ray counts derived from F were quite low.

3. Results

3.1. *Light microscope observations*

The optical microscopic images of the specimens are shown in Fig. 2. After 24 h storage, the optical microscope cross-sectional images showed that discoloration was limited to the surface in the control group (Fig. 2a) and to the dem-

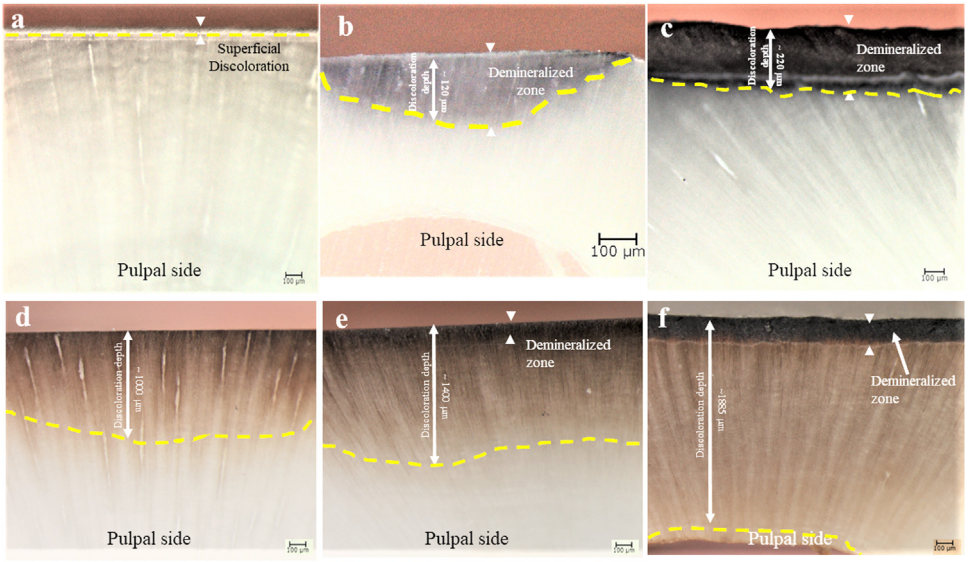

Fig. 2 – Light microscope cross-sectional images of SDF-treated dentin at 3× magnification, (a) sound dentin after 24 h storage; (b) 30 min EDTA-treated dentin after 24 h storage; (c) 13-h EDTA-treated dentin after 24 h storage; (d) sound dentin after 1-year storage; (e) 30 min EDTA-treated dentin after 1-year storage; and, f. 13-h EDTA-treated dentinafter 1-year storage. (Yellow dotted line indicates maximum depth of discoloration) (For interpretation of the references to color in this figure legend, the reader is referred to the web version of this article).

ineralized dentin in the EDTA-treated groups without deeper discoloration (Fig. 2b,2c).

After 2-weeks storage, the discoloration extended to a depth of 720 ± 1.5 µm in all groups other than the 24 h groups. However, after 1-year storage, the depth of visible discoloration in the sound group was recorded at a depth of 1150 ± 2.5 µm (Fig. 2d). The depth of discoloration was greater in the 30 min EDTA-treated dentin group recording a depth of approximately 1400 µm (Fig. 2e). In the 13 h EDTA-treated dentin group, the discoloration depth extended along the whole cross-sectioned surface of the specimens with the demineralized zone recording the darkest color with a gradual decrease in intensity towards the pulp (Fig. 2f).

All dentin groups showed the advancement of discoloration depth through time which was more aggressive in the demineralized dentin groups than the sound dentin group (Fig. 3).

3.2. *SEM/EDS observation*

Observation started 5–10 µm below the surface of the specimen. The morphological analysis after 24 h storage showed multiple spherical particles within the dentinal tubules in the sound dentin (Fig. 4a). However, fewer spherical particles appeared in the 30 min EDTA-treated group (Fig. 4b) while the 13 h EDTA-treated group showed tubules without any deposits (Fig. 4c). After 2-weeks storage, SEM images showed a dramatic decrease in the number of the spherical particles in the sound dentin group (Fig. 4d), while no particles were observed in the 30 min EDTA-treated group (Fig. 4e). The 13 h EDTA-treated group showed crystal-shaped particles within dentinal tubules near the surface (Fig. 4f). After 1-year of storage, a few crystals were observed in the sound dentin group (Fig. 4g). However, in the demineralized dentin groups multiple crystal formations beneath the surface and decreasing in number towards the pulpal direction in the demineralized dentin groups were observed (Fig. 4h and i). The EDS point analysis for the spherical particles that appeared in the sound dentin group and 30 min EDTA-treated dentin group, showed a peak for calcium and a low peak for fluoride which may indicate the particles were calcium fluoride (Fig. 5), as speculated in previous studies [19], while the EDS point analysis for the crystal-shaped particles found in the 13 h EDTA-treated group, showed a high peak for silver suggesting the formation of silver crystals (Fig. 5).

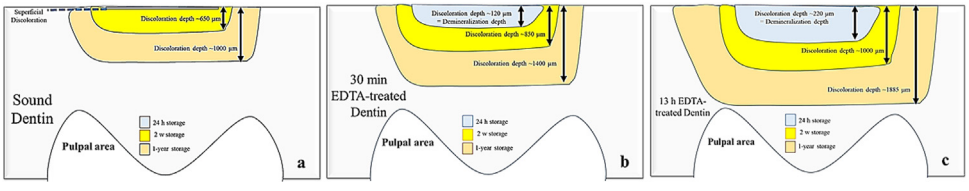

Fig. 3 – Schematic Illustrative diagram summarizing the data obtained from Light microscopic cross-sectional images, (a) Sound dentin, (b) 30 min EDTA-treated dentin; and, (c) 13-h EDTA-treated dentin.

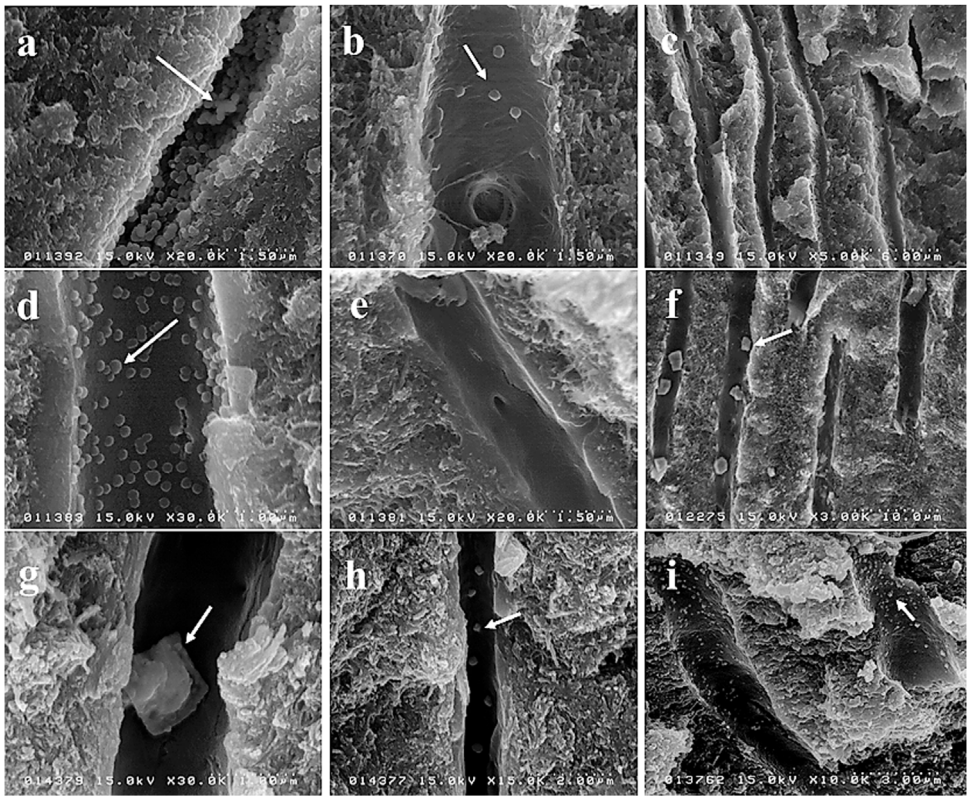

Fig. 4 – Fractured cross-sectional SEM images for SDF-treated dentin, (a) sound dentin after 24 h storage; (b) 30 min EDTA-treated dentin after 24 h storage; (c) 13 h EDTA-treated dentin after 24 h storage; (d) sound dentin after 2-weeks storage; (e) 30 min EDTA-treated dentin after 2-weeks storage; (f) 13 h EDTA-treated dentin after 2-weeks storage; (g) sound dentin after 1-year storage; (h) 30 min EDTA-treated dentin after 1-year storage; and, (i) 13 h EDTA-treated dentin after 1-year storage.

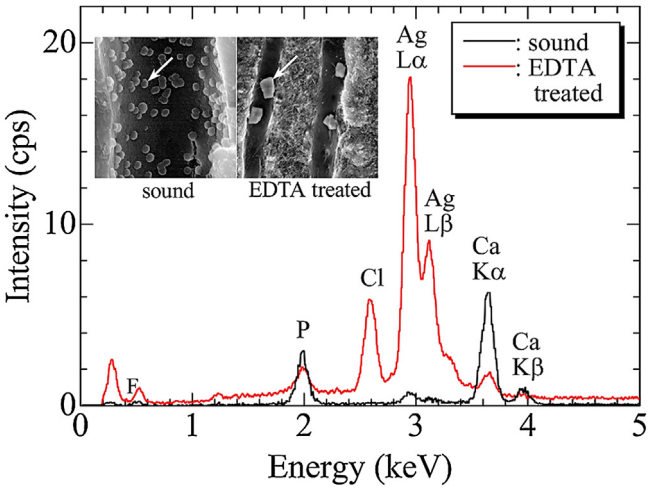

Fig. 5 – EDS point analysis for the spherical particles in sound dentin and 30 min EDTA-treated dentin groups (black) and, crystals in 13 h EDTA-treated dentin group (red). (arrows refer to particles formed within the dentinal tubules) (For interpretation of the references to color in this figure legend, the reader is referred to the web version of this article).

3.3. *EDS line analysis*

The elemental line analysis after 24 h and 2 weeks, could not detect silver in all groups. However, after 1 year of storage the analysis showed silver had penetrated up to 1000 μm into the sound dentin specimens while in the demineralized specimens silver penetrated throughout the whole thickness of the demineralized zone and further penetration into the sound dentin beneath the demineralized zone, reaching a depth around 1750 μm from dentin surface with the highest concentration of silver observed at the junction between demineralized and mineralized dentin zones. (Fig. 6)

3.4. *Micro-PIXE/PIGE analysis*

Fig. 7 shows the typical X(γ)-ray spectra for entire region of analysis. The lower energy spectrum was provided by the Si(Li) detector (Fig. 7A) and the higher energy spectrum was provided by the CdTe detector (Fig. 7B). The characteristic X-rays from P, S, Ca, Zn, and Ag could be identified (Fig. 7A). (Cr and Ni were also detected in the background.) The characteristic X-rays from Ag and the prompt γ-ray from F could be identified (Fig. 7B). The typical elemental distribution images obtained by the element specific X(γ)-rays are shown in Fig. 8 for the 30 min EDTA-treated dentin specimen after 1-year of storage. Sulfur (S) was homogeneously detected throughout the dentin; thus,

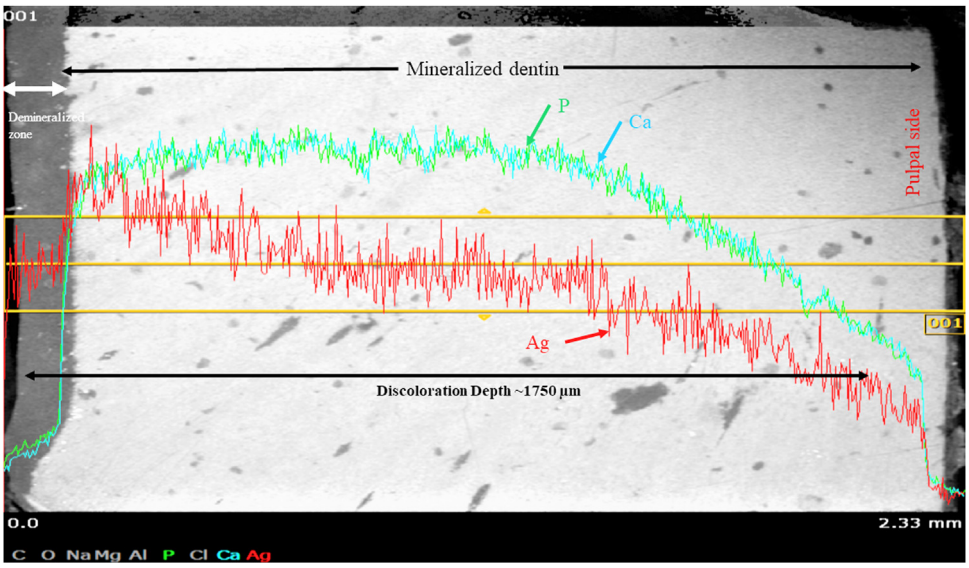

Fig. 6 – EDS line analysis image of the 13 h EDTA-treated dentin with SDF application after 1-year storage.

the specimen shape and the surface layer position could be identified from the image of the S distribution. In comparison with the S and Ca distribution images, demineralization of the surface layer was observed in the Ca image (dotted line), which suggests the loss of surface mineralization. Ag showed a higher concentration at the dentin surface and the concentration gradient that decreased toward the pulpal side was also easily visualized. The prompt γ-ray from F was not very strong, therefore, the distribution image of F was not as clear as for the other elements detected. However, it appeared as is the F was absorbed along the dentin surface.

In order to reveal the depth profile of Ca, Ag, and F, the cumulative profiles were calculated from the elemental distribution images as the function of the X(γ)-ray intensity and the depth from the dentin surface in the 1-year storage group as shown in Fig. 9 for the sound dentin group and Fig. 10 for the demineralized dentin groups. Penetration of Ag and its internal diffusion was clearly shown in the depth profiles of specimens, proving that silver can penetrate the whole thickness of the demineralized zone with further penetration into the underlying mineralized dentin to a total penetration depth of more than 1000 μm.

The Micro-PIXE test showed no noticeable differences in the silver penetration depth among the different storage times (24 h, 2 weeks and 1 year) within the same group, indicating that silver can penetrate deeply once applied and penetration depth is almost not affected by time. The depth profile of F was not as clear as the other element profiles. However, a similar internal diffusion pattern as Ag could be observed.

4. Discussion

The present study evaluated the penetration depth of silver ions into the demineralized and sound dentin using scanning electron microscope-based elemental analysis methods and Micro-focused particle induced X-ray emission (PIXE) and particle induced gamma-ray emission (PIGE) analysis. The results indicated that silver penetrated the demineralized lesion completely with further penetration into the underlying sound dentin. Based on the findings of the current study, the null hypothesis was rejected.

In the current study, bovine teeth were used as a substitute for human teeth, as both human and bovine teeth show good

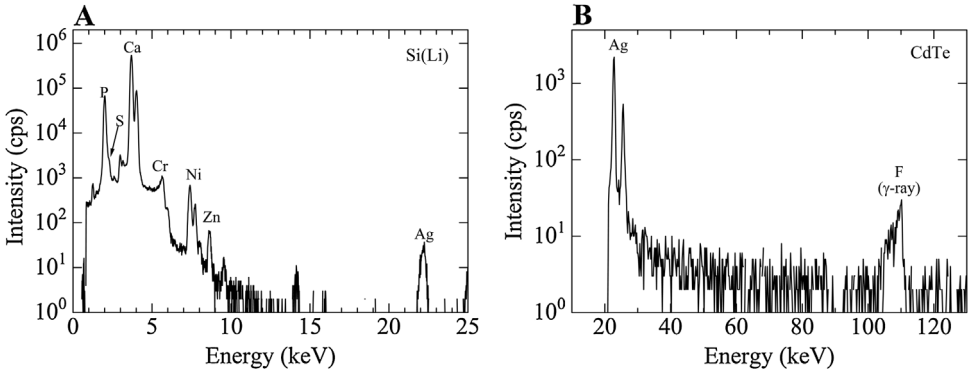

Fig. 7 – Typical X(γ)-ray spectra for the entire specimen obtained by micro PIXE/PIGE, (A) lower energy spectrum provided by the Si(Li) detector. (B) higher energy spectrum provided by the CdTe detector.

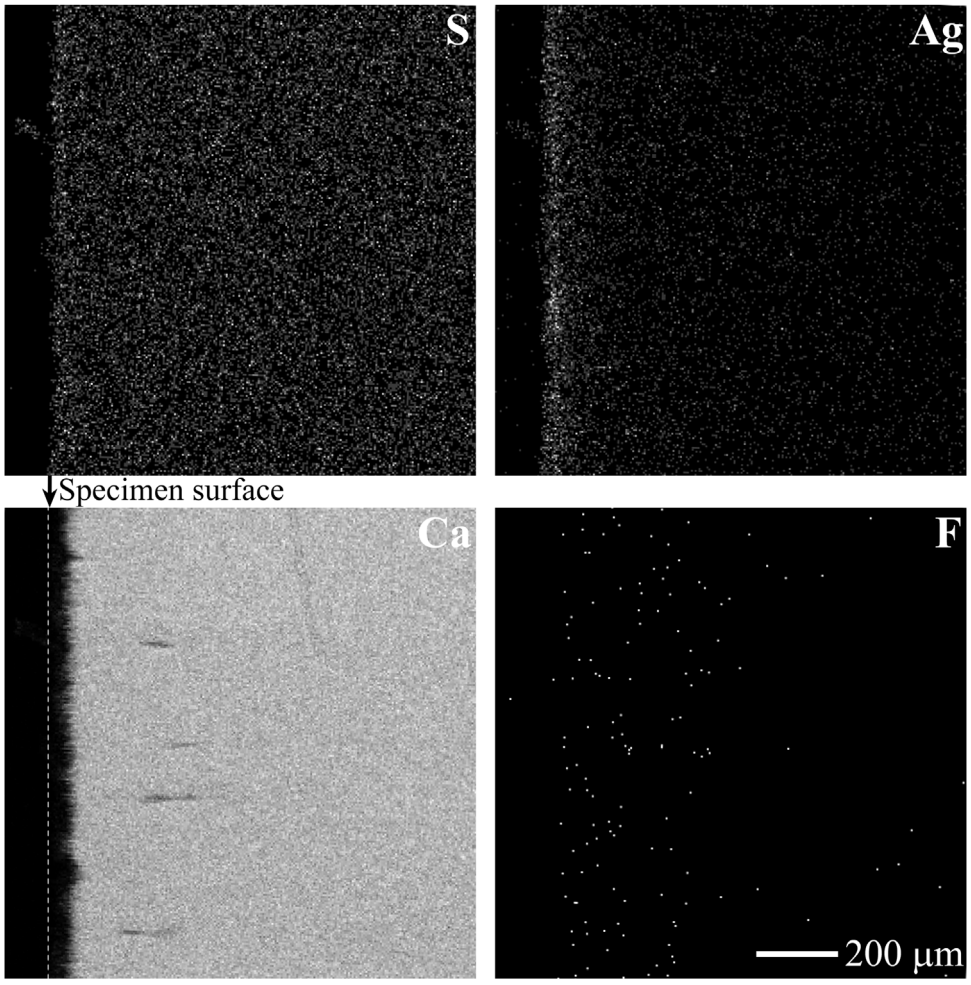

Fig. 8 – Typical micro PIXE/PIGE elemental distribution images obtained by those element specific X(γ)-rays in a 30 min EDTA-treated dentin after 1-year storage.

similarities in structure and chemical composition as human dentin [20].

Ethylene diamine tetra acetic acid (EDTA) is a strong calcium chelating agent which can demineralize the dentin without altering the collagen structural conformation [21]. Optical coherence tomography (OCT) is a non-invasive method with higher sensitivity and specificity than radiographic methods [22]. It has been proven to be a promising method for detecting demineralized dentin lesions [23]. The mean demineralized dentin thicknesses after EDTA treatment measured

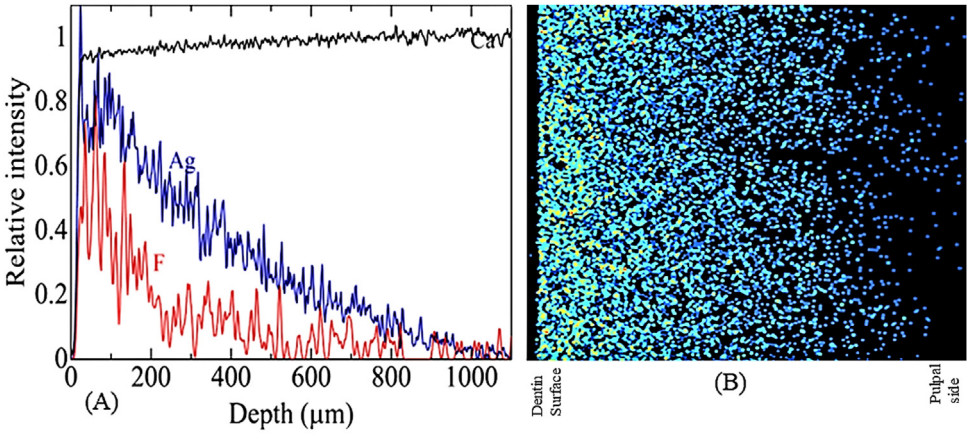

Fig. 9 – (A) Micro-PIXE/PIGE depth profile of Ca, Ag, and F in the sound dentin group after 1-year storage, (B) Elemental distribution of Ag inside sound dentin group after 1-year storage.

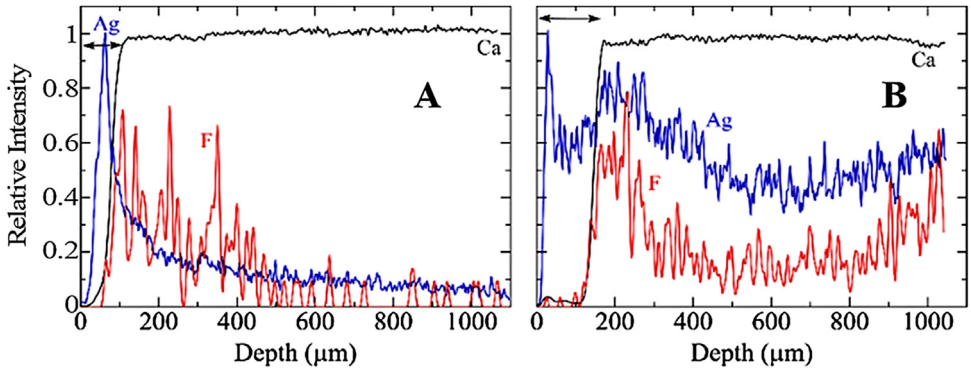

Fig. 10 – Micro-PIXE/PIGE depth profile of Ca, Ag, and F in the demineralized dentin group after 1-year storage, (A) 30 min EDTA-treated dentin group, (B) 13 h EDTA-treated dentin group.

with OCT for 30 min and 13 h were 80 and 200 μm, respectively.

SDF is a colorless topical solution in which its chemical structure [Ag $(NH_3)_2$ F] consists mainly of a diammine silver ion complex [Ag $(NH_3)_2]^+$ and fluoride ions (F^-). When SDF is applied to tooth structures, silver ions are released from the diammine silver ion complex [24]. These silver ions are highly reactive and have a high polarizing power [4], consequently part of the silver ions react with hydroxyapatite forming silver phosphate (Ag_3PO_4) and the other part is reduced by the proteins (collagen) resulting in metallic silver attached to the protein (silver-protein complex). However, the silver phosphate crystals are unstable and reduce to silver ions to form metallic silver [25]. Once formed, silver crystals are round [18] in shape being a few nano-meters in size and by the time the crystals aggregate they form hexagonal- or square-shaped crystals of a sub-micrometer size [26].

A previous study mentioned that silver and fluoride ions from SDF can penetrate from 50 to 200 μm into the dentin. However, the study assessed the "remineralization depth" using a micro-hardness test [27] which is not applicable and not accurate for silver penetration. Willershausen et al mentioned that silver can only penetrate up to 40 μm into the dentin due to the large size of silver crystals [28]. In the current study the depth of silver penetration into sound and demineralized dentin was assessed using light microscopy, SEM, EDS and a micro-PIXE/PIGE test.

The findings of the light microscopy provided images of the discoloration depth which can be regarded as an indicator for the penetration depth of the SDF and therefore of silver penetration. Silver ions released from SDF have a high affinity for protein (collagen), so the more collagen exposed, the more silver uptake, and the faster the color change. Therefore, the greater amount of exposed collagen in demineralized dentin will lead to more silver uptake and its reduction to metallic silver, resulting in a darker color change within a short time. [18]

After 24 h storage, the discoloration was confined to the surface in the control group as silver with higher concentration on the surface was directly exposed to light and heat which will cause rapid reduction of silver ions into crystals [25]. This rapid maturation and deposition of silver crystals will cause a faster color change [11] while crystals inside dentinal tubules may still be nanometer-sized and disperse along the tubules [13]. In the demineralized group the whole thickness of the demineralized dentin zone was discolored because of the rapid reduction of silver ions due to the exposed collagen network [25]. The discoloration started to appear in the intact dentin after 2-weeks storage. However, after 1-year of storage the images showed prominent discoloration that extended along the full thickness of the demineralized zone with discoloration extending into the underlying sound dentin with a gradual decrease in the discoloration intensity as the concentration of the penetrating silver decreased towards the pulp.

Fluoride ions released from SDF will react with hydroxyapatite (HAp) forming calcium fluoride (CaF_2). Calcium fluoride is important because it acts as a temporary reservoir of fluoride ions which release F ions at low pH, promoting remineralization by facilitating formation of fluoroapatite (FAp) [19,29]. Regarding the calcium fluoride formation, the calcium arising from some the dissolution of HAp reacts with fluoride ions to form calcium fluoride which was detected by EDS as globular spherical particles. However, the amount of CaF_2 greatly decreased and disappeared over time as it is easily dissolved [30,25,29].

In the current study, we used different magnifications while observing the surface morphology of the samples to focus on the area of interest and to highlight the differences between different groups. In addition, the high variation in particle size made it more difficult to obtain images with same magnification among different groups. silver could not be detected after 24 h storage using SEMEDS as most of the silver crystals formed were still nanometers in size which was difficult to detect due to the low magnification and resolution of SEMEDS [19,13]. After 2-weeks storage, SEM and EDS point analysis was able to detect silver crystal formation as the silver crystals had coalesced to form sub-micrometer sized crystal formations [11]. However, the depth of penetration could not be assessed using EDS line analysis as the concentration of the deposited silver crystals was still not great enough for detection.

After 1-year of storage, the depth of silver penetration was able to be measured using EDS line analysis, as almost all silver ions were reduced to a mature silver crystal formation. Silver penetration was detected along the whole thickness of demineralized zone with further penetration into the underlying sound dentin.

In this study, micro-PIXE/PIGE was applied for the estimation and visualization of Ag and F (which are component atoms of SDF) and Ca and S (which are component atoms of dentin). PIXE has a higher sensitivity for heavy elements compared with electron microscope derived elemental distribution analytical methods (e.g. SEM/EDS or electron microscope micro-analysis (EPMA)) [31]. In addition, PIGE can detect F with greater sensitivity compared to SEM/EDS. Therefore, the distribution of the above elements could be successfully visualized. Ca distribution images visualized the surface demineralization by EDTA treatment well, and the thickness of the demineralized zone was in good agreement with the light microscope observations. Ag distribution images and depth profiles showed a clear concentration gradient from the dentin surface toward the inner parts of the mineralized dentin. The F images and profiles were not as clear as those for Ag. However, a similar internal diffusion pattern as Ag could be observed. These results suggest the simultaneous penetration of Ag and F derived from SDF with the penetration depths being able to be successfully visualized.

From the current research, silver penetration resulting from SDF application to dentin was deeper than previously reported. The relationship between discoloration and silver penetration depth was also clearly observed. However, the composition of silver deposition remains unclear and further studies are needed to more fully understand the reactions between SDF and dentin.

5. Conclusion

Silver ions can infiltrate demineralized dentin lesion completely with further penetration into the underlying sound dentin. Silver penetrates deeply once applied to dentin while discoloration depth increases with time. Time is a crucial factor for silver maturation and detection. The higher the degree of dentin demineralization the faster the silver deposition rate with deeper depth of penetration.

Acknowledgment

This research was supported by the Japan Society for the Promotion of Science (16H05515). There is no conflict of interest in this study. Micro-PIXE analyses were supported by the Joint-use Research Facility for Collaborative Project with NIRS-PASTA (2018-001) of the National Institute of Radiological Sciences (NIRS, Japan).

Appendix A. Supplementary data

Supplementary material related to this article can be found, in the online version, at doi:https://doi.org/10.1016/j.dental.2019.08.111.

REFERENCES

[1] Deb S, Chana S. Biomaterials in relation to dentistry. Front Oral Biol 2015;17:1–12.
[2] Massa MA, Covarrubias C, Bittner M, Fuentevilla IA, Capetillo P, Von Marttens A, et al. Synthesis of new antibacterial composite coating for titanium based on highly ordered nanoporous silica and silver nanoparticles. Mater Sci Eng C Mater Biol Appl 2014;45:146–53.
[3] Peng JJ, Botelho MG, Matinlinna JP. Silver compounds used in dentistry for caries management: a review. J Dent 2012;40:531–41.
[4] Rosenblatt A, Stamford TC, Niederman R. Silver diamine fluoride: a caries šilver-fluoride bullet:. J Dent Res 2009;88:116–25.
[5] Suzuki T, Nishida M, Sobue S, Moriwaki Y. Effects of diammine silver fluoride on tooth enamel. J Osaka Univ Dent Sch 1974;14:61–72.
[6] Delbem AC, Bergamaschi M, Sassaki KT, Cunha RF. Effect of fluoridated varnish and silver diamine fluoride solution on enamel demineralization: pH-cycling study. J Appl Oral Sci 2006;14:88–92.
[7] Chu CH, Mei L, Seneviratne CJ, Lo EC. Effects of silver diamine fluoride on dentine carious lesions induced by Streptococcus mutans and Actinomyces naeslundii biofilms. Int J Paediatr Dent 2012;22:2–10.
[8] Percival SL, Hill KE, Williams DW, Hooper SJ, Thomas DW, Costerton JW. A review of the scientific evidence for biofilms in wounds. Wound Repair Regen 2012;20:647–57.
[9] Sharma G, Puranik MP, K RS. Approaches to arresting dental caries: an update. J Clin Diagn Res 2015;9. ZE08-11.
[10] Schwendicke F, Gostemeyer G. Cost-effectiveness of root caries preventive treatments. J Dent 2017;56:58–64.
[11] Sayed M, Matsui N, Hiraishi N, Nikaido T, Burrow MF, Tagami J. Effect of glutathione bio-molecule on tooth discoloration associated with silver diammine fluoride. Int J Mol Sci 2018;19, http://dx.doi.org/10.3390/ijms19051322.
[12] Rossi G, Squassi A, Mandalunis P, Kaplan A. Effect of silver diamine fluoride (SDF) on the dentin-pulp complex: ex vivo histological analysis on human primary teeth and rat molars. Acta Odontol Latinoam 2017;30:5–12.
[13] Mei ML, Ito L, Cao Y, Lo EC, Li QL, Chu CH. An ex vivo study of arrested primary teeth caries with silver diamine fluoride therapy. J Dent 2014;42:395–402.
[14] Thanatvarakorn O, Islam MS, Nakashima S, Sadr A, Nikaido T, Tagami J. Effects of zinc fluoride on inhibiting dentin demineralization and collagen degradation in vitro: a comparison of various topical fluoride agents. Dent Mater J 2016;35:769–75.
[15] Sugiyama T, Uo M, Wada T, Hongo T, Omagari D, Komiyama K, et al. Novel metal allergy patch test using metal nanoballs. J Nanobiotechnol 2014;12, 51-014-0051-7.
[16] Sugiyama T, Uo M, Wada T, Omagari D, Komiyama K, Miyazaki S, et al. Detection of trace metallic elements in oral lichenoid contact lesions using SR-XRF, PIXE, and XAFS. Sci Rep 2015;5:10672.
[17] Komatsu H, Yamamoto H, Matsuda Y, Kijimura T, Kinugawa M, Okuyama K, et al. Fluorine analysis of human enamel around fluoride-containing materials under different pH-cycling by μ-PIGE/PIXE system. Nucl Instrum Methods Phys Res Sect B 2011;269:2274–7.
[18] Sayed M, Matsui N, Hiraishi N, Inoue G, Nikaido T, Burrow MF, et al. Evaluation of discoloration of sound/demineralized root dentin with silver diamine fluoride: in-vitro study. Dent Mater J 2018.
[19] Mei ML, Ito L, Cao Y, Li QL, Lo EC, Chu CH. Inhibitory effect of silver diamine fluoride on dentine demineralisation and collagen degradation. J Dent 2013;41:809–17.
[20] Teruel Jde D, Alcolea A, Hernandez A, Ruiz AJ. Comparison of chemical composition of enamel and dentine in human, bovine, porcine and ovine teeth. Arch Oral Biol 2015;60:768–75.

[21] Kim DS, Park SH, Choi GW, Choi KK, Kim SY. Effect of EDTA treatment on the hybrid layer durability in total-etch dentin adhesives. Dent Mater J 2011;30:717–22.
[22] Shimada Y, Sadr A, Sumi Y, Tagami J. Application of optical coherence tomography (OCT) for diagnosis of caries, cracks, and defects of restorations. Curr Oral Health Rep 2015;2:73–80.
[23] Shimada Y, Nakagawa H, Sadr A, Wada I, Nakajima M, Nikaido T, et al. Noninvasive cross-sectional imaging of proximal caries using swept-source optical coherence tomography (SS-OCT) in vivo. J Biophotonics 2014;7:506–13.
[24] Mei ML, Li QL, Chu CH, Yiu CK, Lo EC. The inhibitory effects of silver diamine fluoride at different concentrations on matrix metalloproteinases. Dent Mater 2012;28:903–8.
[25] Lou YL, Botelho MG, Darvell BW. Reaction of silver diamine [corrected] fluoride with hydroxyapatite and protein. J Dent 2011;39:612–8.
[26] Hou WC, Stuart B, Howes R, Zepp RG. Sunlight-driven reduction of silver ions by natural organic matter: formation and transformation of silver nanoparticles. Environ Sci Technol 2013;47:7713–21.
[27] Chu CH, Lo EC. Microhardness of dentine in primary teeth after topical fluoride applications. J Dent 2008;36:387–91.
[28] Willershausen I, Schulte D, Azaripour A, Weyer V, Briseño B, Willershausen B. Penetration potential of a silver diamine fluoride solution on dentin surfaces. An ex vivo study. Clin Lab 2015;61:1695–701.
[29] Zhao IS, Mei ML, Burrow MF, Lo EC, Chu CH. Prevention of secondary caries using silver diamine fluoride treatment and casein phosphopeptide-amorphous calcium phosphate modified glass-ionomer cement. J Dent 2017;57:38–44.
[30] McCann HG. The solubility of fluorapatite and its relationship to that of calcium fluoride. Arch Oral Biol 1968;13:987–1001.
[31] Campbell JL, Teesdale WJ, Halden NM. Theory practice and application of micro-PIXE analysis and element-distribution maps. Can Mineral 1995;33:279–92.